Article

Calorimetric Thermoelectric Gas Sensor for the Detection of Hydrogen, Methane and Mixed Gases

Nam-Hee Park, Takafumi Akamatsu, Toshio Itoh, Noriya Izu and Woosuck Shin *

National Institute of Advanced Industrial Science and Technology (AIST), Shimo-Shidami, Moriyama-ku, Nagoya 4638560, Japan; E-Mails: namhee.park@aist.go.jp (N.-H.P.); t-akamatsu@aist.go.jp (T.A.); itoh-toshio@aist.go.jp (T.I.); n-izu@aist.go.jp (N.I.)

* Author to whom correspondence should be addressed; E-Mail: w.shin@aist.go.jp; Tel.: +81-527-367-107; Fax: +81-527-367-244.

Abstract: A novel miniaturized calorimeter-type sensor device with a dual-catalyst structure was fabricated by integrating different catalysts on the hot (Pd/θ-Al_2O_3) and cold (Pt/α-Al_2O_3) ends of the device. The device comprises a calorimeter with a thermoelectric gas sensor (calorimetric-TGS), combining catalytic combustion and thermoelectric technologies. Its response for a model fuel gas of hydrogen and methane was investigated with various combustor catalyst compositions. The calorimetric-TGS devices detected H_2, CH_4, and a mixture of the two with concentrations ranging between 200 and 2000 ppm at temperatures of 100–400 ℃, in terms of the calorie content of the gases. It was necessary to reduce the much higher response voltage of the TGS to H_2 compared to CH_4. We enhanced the H_2 combustion on the cold side so that the temperature differences and response voltages to H_2 were reduced. The device response to H_2 combustion was reduced by 50% by controlling the Pt concentration in the Pt/α-Al_2O_3 catalyst on the cold side to 3 wt%.

Keywords: calorimeter; thermoelectric gas sensor; dual catalyst; methane; hydrogen

1. Introduction

Gas calorimeters, which measure the calorific values or Wobbe Index (WI) of gases [1], are used to control the thermal input in various types of steel mill and petrochemical industry furnaces, as well as control the fuel in power plant turbines. Conventional calorimeters for fuel gas, natural gas, or coal

gasification products are highly complex, sophisticated apparatus for monitoring the heats of combustion of fuels in the burners or turbines of power plants [2]. Typical calorimeters are large, self-standing units that are used to monitor large-scale systems, and there are no smaller calorimeters appropriate for the various burners or turbines of smaller-scale systems.

A new sensor device is presented in this study which contains all the functional elements of a conventional thermocouple-type calorimeter (temperature sensor, catalytic combustor, and heater). The device, essentially a calorimeter of a thermoelectric gas sensor (calorimetric-TGS), combines catalytic combustion and thermoelectric technologies [3]. The sensor is suitable for low-cost production and advantageous in terms of short start-up and response times [4]. Detailed features of thermoelectric sensor technologies have been described previously [5].

Natural gas consists mostly of methane, along with lesser amounts of ethane and propane. Noncombustible components such as carbon dioxide and nitrogen may also be present. Several reports have described the typical compositions of natural gas [6]. In the case of coal gas, the principal component, CO, is reacted with H_2O and produced to H_2 and CO_2 before the gas flows into the burner or turbine [7].

Considering fuel gas compositions, TGS sensors must be able to properly combust H_2, CO and CH_4. The detection of H_2 and CO by TGS has been demonstrated previously [3,8], but the detection of CH_4 is challenging as it requires a higher catalyst temperature [9]. At lower catalyst temperatures, the heat of combustion catalyst for H_2 exceeds that of CH_4, causing the ratio of combustion heat to sensor output to deviate significantly from linearity.

In the present study, we integrated modified catalytic combustors for CH_4 to balance the combustion calories-to-sensor outputs for more reliable calorimetric applications. The fabrication, characterization, and gas responses of the micro calorimetric-TGS devices, which utilize a thermoelectric thin film, were investigated with various catalytic combustor material sets and operating temperatures. The responses of the TGS to the combustion heat for different compositions of gases were also investigated.
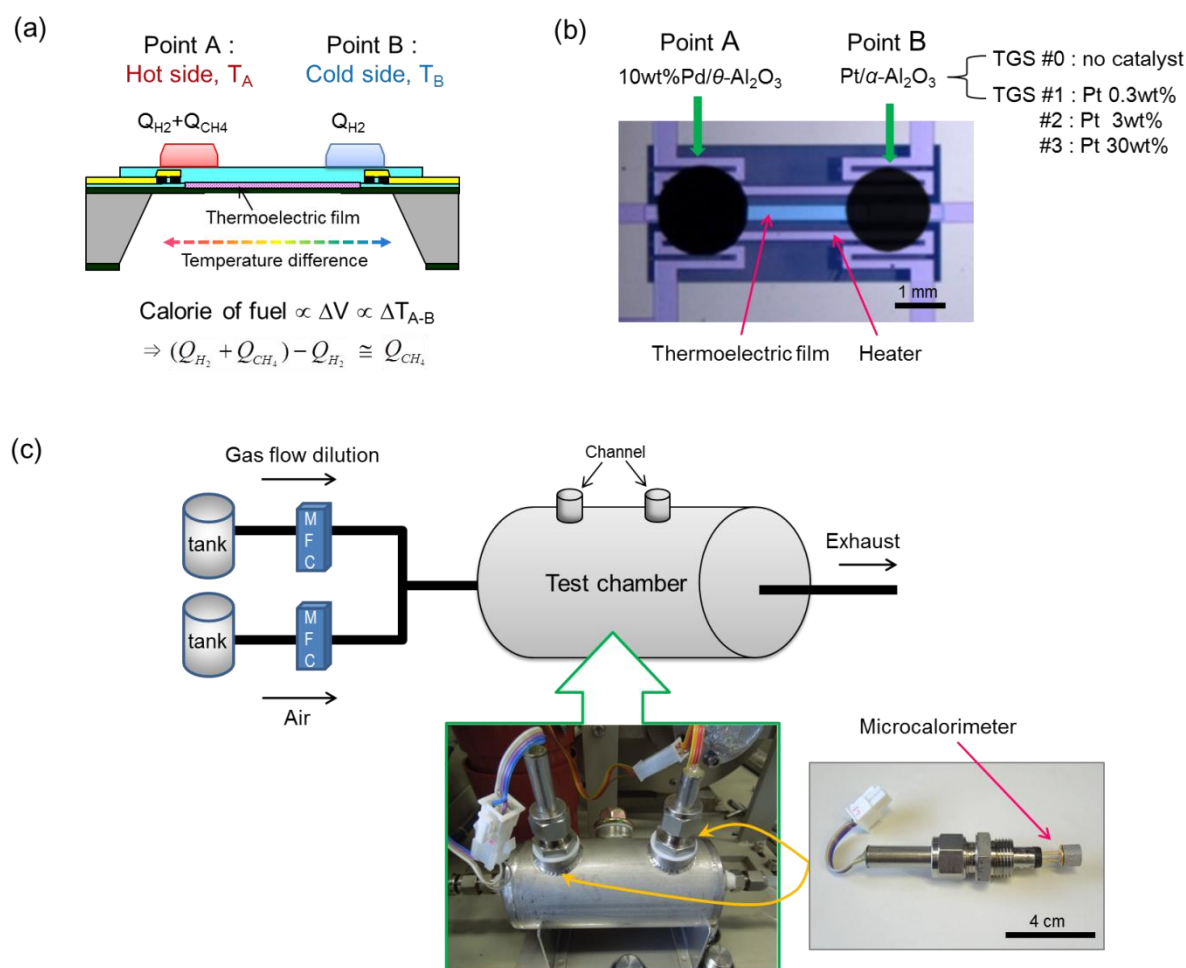
2. Experimental Section

2.1. Structure and Working Principle of the Dual-Catalyst Calorimetric-TGS Devices

Our purpose was to design and demonstrate a calorimetric-TGS with a dual-catalyst structure to balance the combustion calories for H_2 and CH_4 in a gas fuel. To this end, Pd/θ-Al_2O_3 and Pt/α-Al_2O_3 were deposited on the hot (point A) and cold (point B) sides of a membrane, respectively, as depicted in Figure 1a. The Pd/θ-Al_2O_3 catalyst oxidizes both H_2 and CH_4 gases well, and the Pt/α-Al_2O_3 catalyst is the most well-known catalytic combustor for hydrogen, with high activity toward its selective oxidation. The role of the Pt/α-Al_2O_3 catalyst at point B is to improve the heat of H_2 catalytic combustor (Q_{H_2}) on the cold side and to reduce the temperature difference between the hot and cold sides. The structure and working principle of the dual-catalyst calorimetric-TGS are based on our previous study of a micro-thermoelectric hydrogen sensor (micro-THS) with a dual catalyst for H_2 and CO [10]. When a mixture of H_2 and CH_4 is introduced into the calorimetric-TGS device, the Pd/θ-Al_2O_3 catalyst releases the heats of combustion for H_2 and CH_4 ($Q_{H_2} + Q_{CH_4}$) on the hot side (point A), and the heat of combustion of H_2 (Q_{H_2}) is generated by combustion on the Pt/α-Al_2O_3 catalyst on the cold

side (point B). A temperature difference is developed between points A and B, which is then converted into a voltage by the Seebeck effect across the thermoelectric film. Therefore, the combustion heat (Q_{CH_4}) can be obtained by subtracting the combustion heat for H_2 on the $Pt/\alpha\text{-}Al_2O_3$ catalyst at point B (Q_{H_2}) from the total combustion heat for both H_2 and CH_4 on the $Pd/\theta\text{-}Al_2O_3$ catalyst ($Q_{H_2} + Q_{CH_4}$) at point A.

Figure 1. (**a**) Schematic illustration of device structure and working principle, and (**b**) photograph of a calorimetric-TGS device. (**c**) Schematic and photograph of the measurement system for the calorimetric-TGS devices.

2.2. Preparation of Calorimetric-TGS Devices with Various Catalytic Combustors

The size of the calorimetric-TGS chip was 4×4 mm^2, and a double-sided polished Si wafer with 0.35 mm thickness was used as substrate. A silicon-germanium (SiGe) thin film [11] was deposited by DC magnetron sputtering and patterned into the thermoelectric (TE) element by RIE etching. The membrane was designed to be 1.2×0.8 mm^2. The membrane and catalytic combustors of the calorimetric-TGS were fabricated based on our previous studies [5]. The combustion catalysts for the devices were prepared by the colloidal method. For the $Pd/\theta\text{-}Al_2O_3$ catalyst powder, commercially available $\theta\text{-}Al_2O_3$ powder (Taimei Chemicals Co., Ltd., Nagano, Japan; average particle size: 14 nm) was added into 4 wt% Pd-PVP colloids (Pd colloids stabilized in poly(*N*-vinyl-2-pyrrolidone (PVP); Tanaka Precious Metals Co., Ltd., Tokyo, Japan; average Pd nanoparticle size: 4 nm) with mechanical

stirring. Analogously, the Pt/α-Al$_2$O$_3$ catalyst powder was prepared by mixing commercially available α-Al$_2$O$_3$ powder (Taimei; avg. particle size: 100 nm) with 4 wt% Pt-PVP colloid (Pt colloids stabilized in PVP; Tanaka; avg. Pt nanoparticle size: 2 nm). The Pd concentration was fixed at 10 wt% and the Pt concentration was varied from 0.3 to 30 wt%. Each mixture was stirred at 80 ℃ for 1 h. The obtained catalyst pastes were dried in an oven at 90 ℃ for 30 min and subsequently heated at 300 ℃ for 2 h in air. The catalysts powders were mixed with an organic vehicle, *i.e.*, a 9:1 w/w mixture of terpineol and ethyl cellulose, to prepare the dispensing pastes. The pastes were deposited on points A and B of the calorimetric-TGS devices by a dispenser system (Musashi Engineering, Inc., Aichi, Japan), as shown in the photograph in Figure 1b. The thicknesses of the Pd/θ-Al$_2$O$_3$ and Pt/α-Al$_2$O$_3$ catalysts were controlled to be about 25 and 3 μm, respectively. The deposited catalyst pastes were heated at 300 ℃ for 2 h in air. The compositions and names of the prepared devices with the various catalytic combustors are given in Table 1.

Table 1. Calorimetric-TGS devices with various catalytic combustor compositions.

Device	Catalyst	
	Point A	Point B
Calorimetric-TGS #0	10 wt% Pd/θ-Al$_2$O$_3$	No catalyst
Calorimetric-TGS #1	10 wt% Pd/θ-Al$_2$O$_3$	0.3 wt% Pt/α-Al$_2$O$_3$
Calorimetric-TGS #2	10 wt% Pd/θ-Al$_2$O$_3$	3 wt% Pt/α-Al$_2$O$_3$
Calorimetric-TGS #3	10 wt% Pd/θ-Al$_2$O$_3$	30 wt% Pt/α-Al$_2$O$_3$

2.3. Characterization, Gas Response Testing and Combustion Heat

The catalyst surface temperatures on the calorimetric-TGS devices were monitored by IR camera (LAIRD-270A, Nikon, Tokyo, Japan) and the power consumption was estimated from surface temperature. The emissivity of the catalyst was considered and calibrated before the measurement. The combustion performance of the calorimetric-TGS devices was investigated in a gas-flow type test chamber, as shown in Figure 1c. The voltage signals from the devices were recorded with a digital multimeter/data acquisition system (Model 2700, Keithley Instruments, Cleveland, OH, USA) by flowing CH$_4$, H$_2$, and a CH$_4$ + H$_2$ gas mixture at a rate of 200 mL/min in the test chamber (2% CH$_4$/N$_2$ and 2% H$_2$/N$_2$ standard gases; DAIWA Shokai Co., Ltd., Osak, Japan). The voltage signal, ΔV, is considered as an index of the combustion performance of the catalyst in the calorimetric-TGS device, and is evaluated as follows:

$$\Delta V = \alpha \cdot \Delta T \tag{1}$$

where ΔV is the voltage signal, α is Seebeck coefficient of the thermoelectric film, and ΔT is the temperature difference between points A and B, as shown in the Figure 1a and b. The response voltage (ΔV) of a calorimetric-TGS device for gas combustion is defined as the difference between the voltage output of the inflammable gas in air (V_{gas}) and the offset voltage in air (V_{air}), which is given by the follow formula:

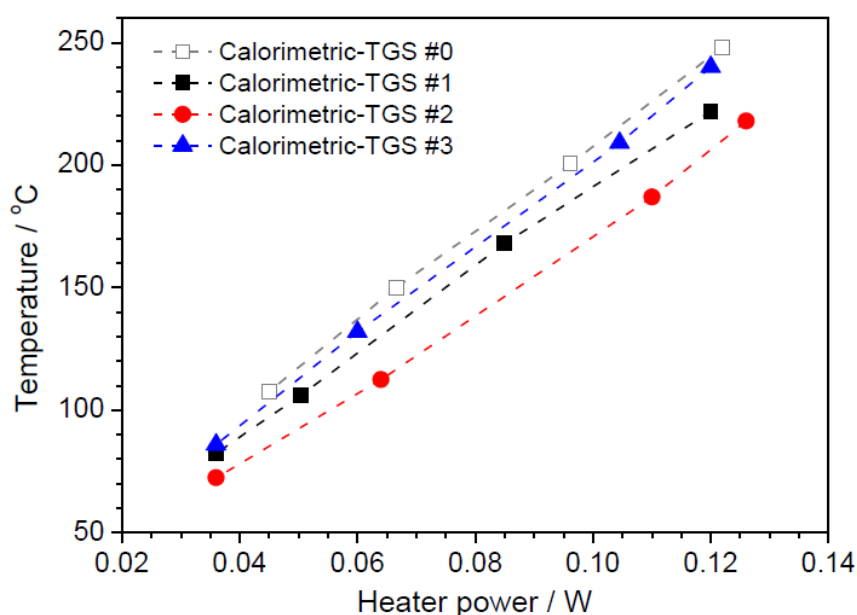$$\Delta V = V_{gas} - V_{air} \tag{2}$$

Finally, the combustion heats of the gas fuels were calculated for the calorimetric-TGS devices.

3. Results and Discussion

3.1. Power Consumption

The surface temperatures of the Pd/θ-Al$_2$O$_3$ catalysts in the calorimetric-TGS devices were determined by monitoring with the IR camera. Figure 2 shows the catalyst temperatures in the range 50−250 ℃ estimated from the surface temperatures as a function of the power consumption of the devices. For devices #0, #1, #2 and #3, the power consumptions display good linearity, requiring 0.122, 0.12, 0.126 and 0.12 W to heat the catalysts to 248, 222, 218 and 240 ℃, respectively.

Figure 2. Catalyst temperature as a function of power consumption, as estimated from the integrated catalyst surface by IR camera monitoring.
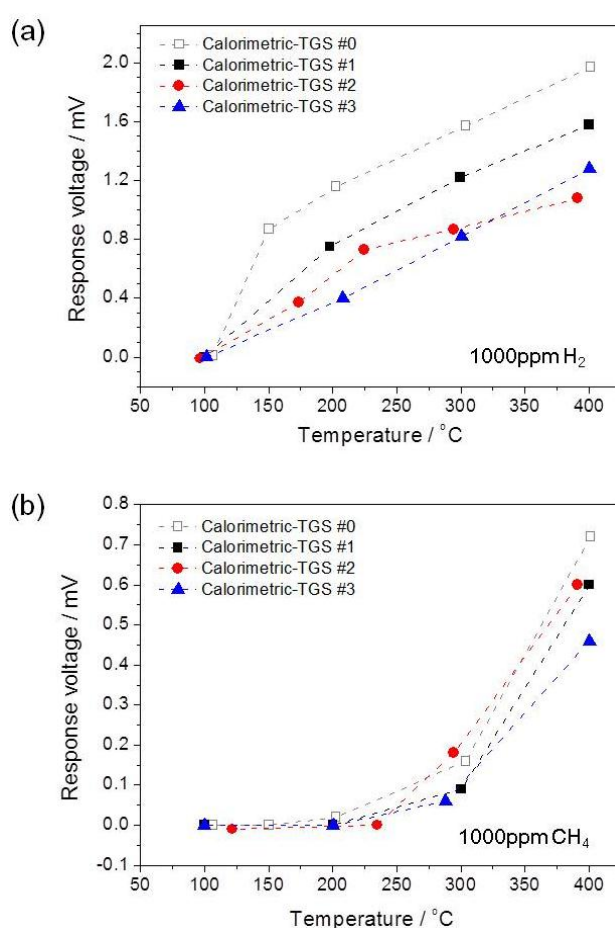

3.2. Combustion Performance with H$_2$, CH$_4$ and the Mixed Gases

Figure 3 shows the temperature dependence of the response voltages ΔV of the devices in the temperature range 100–400 ℃ for flows of (a) 1000 ppm H$_2$ and (b) 1000 ppm CH$_4$ in air. The calorimetric-TGS devices display linear relationships between the temperature increases and the response voltages to H$_2$, except for the device #2. As the Pt concentration in the Pt/α-Al$_2$O$_3$ catalyst at point B increases, the ΔV for H$_2$ of the device decreases in the low temperature range below 250 ℃, as shown in Figure 3a. This result indicates that the H$_2$ combustion performance of the Pt/α-Al$_2$O$_3$ catalyst improves by increasing the Pt concentration. The temperature differences between the Pd and Pt catalysts decrease due to the active combustion by the Pt/α-Al$_2$O$_3$ catalysts with higher Pt concentrations at point B, consequently, ΔV of devices decreases. However, at temperatures over 300 ℃, the combustion performance on point B of device #2, containing 3 wt% Pt/α-Al$_2$O$_3$, becomes lower

than that of the other devices. The response voltage of the calorimetric-TGS #2 at 291 ℃ is close to that of calorimetric-TGS #3 with 30 wt% Pt/α-Al$_2$O$_3$ at 300 ℃. Device #2 subsequently shows the lowest ΔV of 1.08 mV at 391 ℃, indicating the high combustion of H$_2$ on the 3 wt% Pt/α-Al$_2$O$_3$ catalyst. At 400 ℃, the response voltages of devices #0, #1 and #3 are 1.97, 1.58 and 1.28 mV, respectively. It indicates that the catalytic activity and H$_2$ selectivity of the 3 wt% Pt/α-Al$_2$O$_3$ catalyst is higher than those of the 30 wt% Pt/α-Al$_2$O$_3$ catalyst at B point, and the study for the catalytic performance of Pt/alumina catalysts with the various concentration of Pt confirms previously reported results [12].

Figure 3. Temperature dependence of the response voltages ΔV over the temperature range 100–400 ℃ for (**a**) 1000 ppm H$_2$ and (**b**) 1000 ppm CH$_4$ in air.
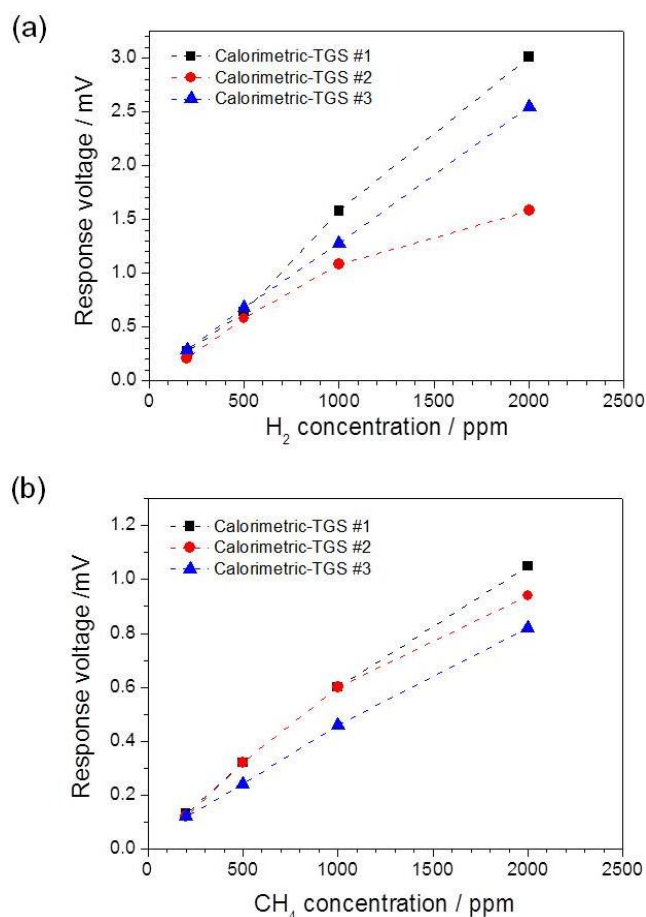

In contrast, the catalysts of the calorimetric-TGS devices start to burn 1000 ppm CH$_4$ at temperatures over 200 ℃, as shown in Figure 3b. The ΔV for 1000 ppm CH$_4$ for devices #0, #1, #2 and #3 are 0.16, 0.09, 0.18 and 0.06 mV at 303, 300, 294 and 288 ℃, respectively. At temperatures over 300 ℃, the calorimetric-TGS #1 shows a rapid increase in ΔV to 0.6 mV at 400 ℃. The combustion performance of the 0.3 wt% Pt/α-Al$_2$O$_3$ catalyst at point B is significantly lower than that of the 10 wt% Pd/θ-Al$_2$O$_3$ catalyst at point A at high temperatures for calorimetric-TGS #1, compared to those of devices #2 and #3. However, device #3 shows the lowest response voltage to CH$_4$ (0.46 mV) at 400 ℃, indicating its high CH$_4$ combustion performance. Furthermore, the 30 wt% Pt/α-Al$_2$O$_3$ catalyst at point B in device #3 has higher CH$_4$ combustion performance than the 3 wt% catalyst in device #2. Device

#0 is no longer tested in following sections and we will discuss only the combustion performance of the devices with dual catalyst, because it confirms the worst combustion performance to H_2 and CH_4 of device #0 compared to other calorimetric-TGS devices in Figure 3.

The response voltages of the devices as a function of H_2 and CH_4 concentrations are shown in Figure 4. The operating temperatures for the calorimetric-TGSs #1, #2 and #3 were 400, 391 and 400 ℃, respectively, and the introduced H_2 and CH_4 concentrations varied from 200 to 2000 ppm in air. The calorimetric-TGS devices show linear relationships between ΔV and the gas concentrations over the gas concentration ranges 200–1000 ppm for both H_2 and CH_4, as shown in Figure 4a and b, respectively. For H_2 combustion performance *versus* gas concentration, the calorimetric-TGS #2 shows a lower ΔV than the other devices (Figure 4a). This means that the 3 wt% Pt/α-Al_2O_3 catalyst in device #2 burns H_2 much better than the other Pt/α-Al_2O_3 catalyst compositions upon increasing gas concentration at 391 ℃. However, the 3 wt% Pt/α-Al_2O_3 catalyst in device #2 did not exhibit a high CH_4 combustion performance; in this case, the 30 wt% catalyst in device #3 performed better, giving the lowest ΔV among the devices (Figure 4b).

Figure 4. Response voltage ΔV as a function of gas concentration for (**a**) H_2 and (**b**) CH_4. The operating temperatures of the calorimetric-TGSs #1, #2 and #3 were 400, 391 and 400 ℃, respectively.

The temperature dependence of ΔV with 1000 ppm mixed gas (H_2:CH_4 = 50:50) for the three devices in the temperature range 100–400 ℃ is shown in Figure 5a. Here, ΔV increases linearly with temperature. The calorimetric-TGS #2 shows lower response voltages than devices #1 and #3: 0.46 mV

at 294 ℃ and 0.7 mV at 391 ℃. This indicates that the H_2 combustion performance of the 3 wt% Pt/α-Al$_2$O$_3$ is much higher than that for CH$_4$ in the mixed gas for the calorimetric-TGS #2, although the Pt/α-Al$_2$O$_3$ catalyst of device #3 has a higher Pt concentration than device #2. The combustion performance toward H_2 at point B with the 3 wt% Pt/α-Al$_2$O$_3$ catalyst seems to be enhanced over the 30 wt% catalyst.

Figure 5. (**a**) Temperature dependence of the response voltage ΔV to 1000 ppm mixed gases (500 ppm CH$_4$ + 500 ppm H$_2$) in air over the temperature range 100–400 ℃. (**b**) ΔV as a function of the mixed gas concentration at 400, 391 and 400 ℃ for devices #1, #2 and #3. (**c**) The estimated ΔV to the mixed gases, calculated from the experimental data for the response voltages to H$_2$ and CH$_4$ from Figure 4, using the formula: [(ΔV to H$_2$) + (ΔV to CH$_4$)]/2.
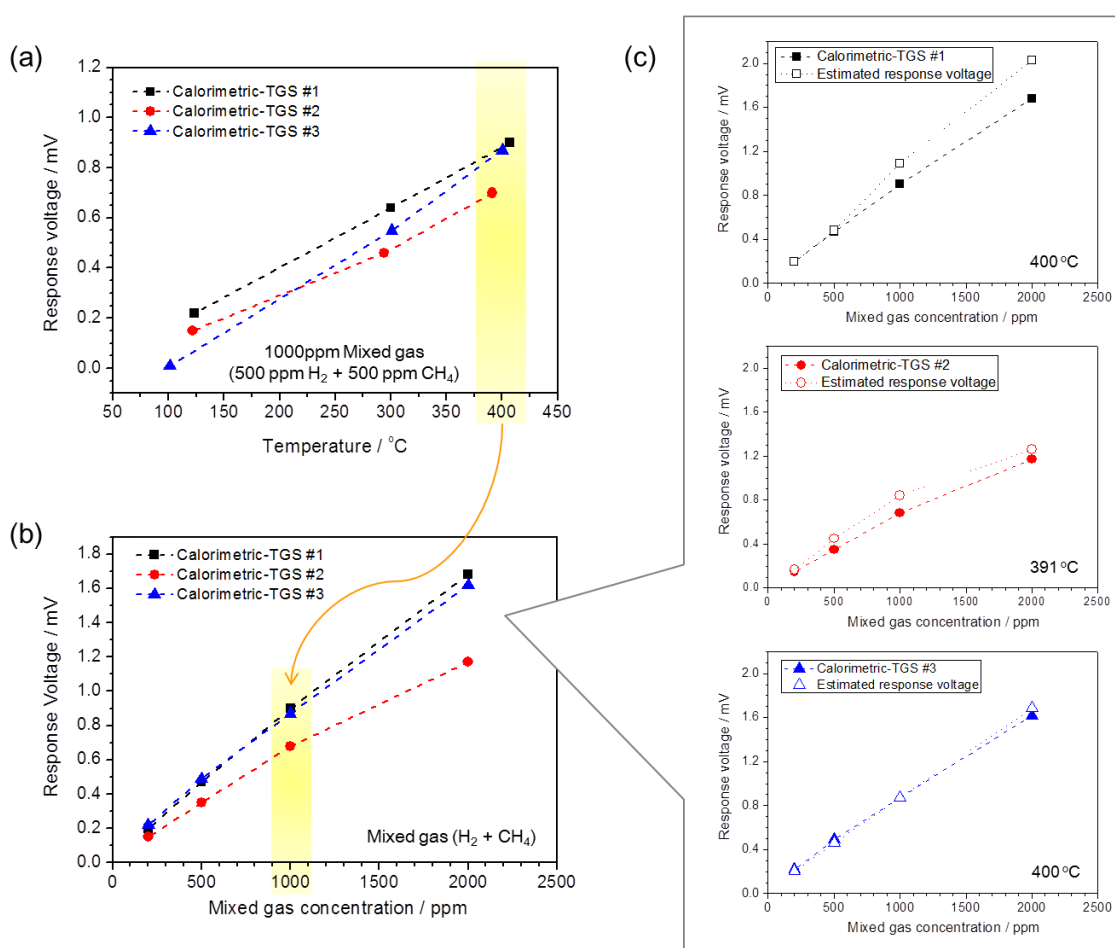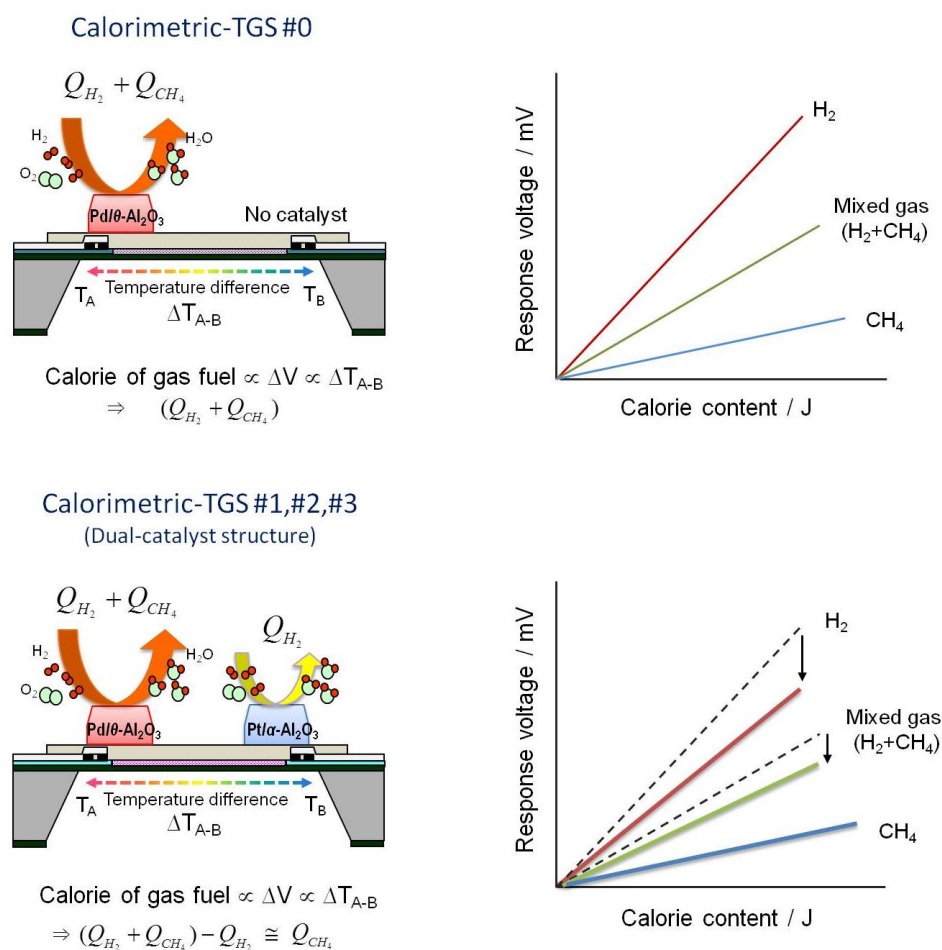

Figure 5b shows the ΔV to the mixed gases for the calorimetric-TGS devices as a function of gas concentration. The operating temperatures for the calorimetric-TGSs #1, #2 and #3 are 400, 391 and 400 ℃, respectively, and the mixed gas concentration (H$_2$:CH$_4$ = 50:50) is varied from 200 to 2000 ppm in air. The ΔV is proportional to the mixed gas concentration for the calorimetric-TGS devices. These results are compared (Figure 5c) to the estimated response voltages, calculated using [(ΔV to H$_2$) + (ΔV to CH$_4$)]/2 with the experimental data from the response voltages to H$_2$ and CH$_4$.

These findings confirm that the gas concentration-dependent response voltages to the mixed gases for the calorimetric-TGS devices correspond well to the estimated response voltages.

Figure 6 shows a schematic illustration of the combustion mechanism of the dual-catalyst calorimetric-TGS devices for mixed H_2 and CH_4 in air, and the expected graphs of gas calorie contents to response voltages. When the mixed gases flow, the calorimetric-TGS #0 device combusts both H_2 and CH_4, and a temperature difference is developed between points A and B due to the heats of combustion ($Q_{H_2} + Q_{CH_4}$) of both H_2 and CH_4 at point A (top left, Figure 6). For this device, a graph of the expected gas calorie-to-response voltage is shown in the top right of Figure 6. On the other hand, in the dual-catalyst calorimetric-TGS devices #1–3, the temperature differences between points A and B can be reduced by lowering the excessive heats of combustion due to H_2 (Q_{H_2}), to balance with the heats of CH_4 combustion (Q_{CH_4}). Therefore, the gas calorie-to-response voltage graph can be expected as shown in the bottom right of Figure 6.
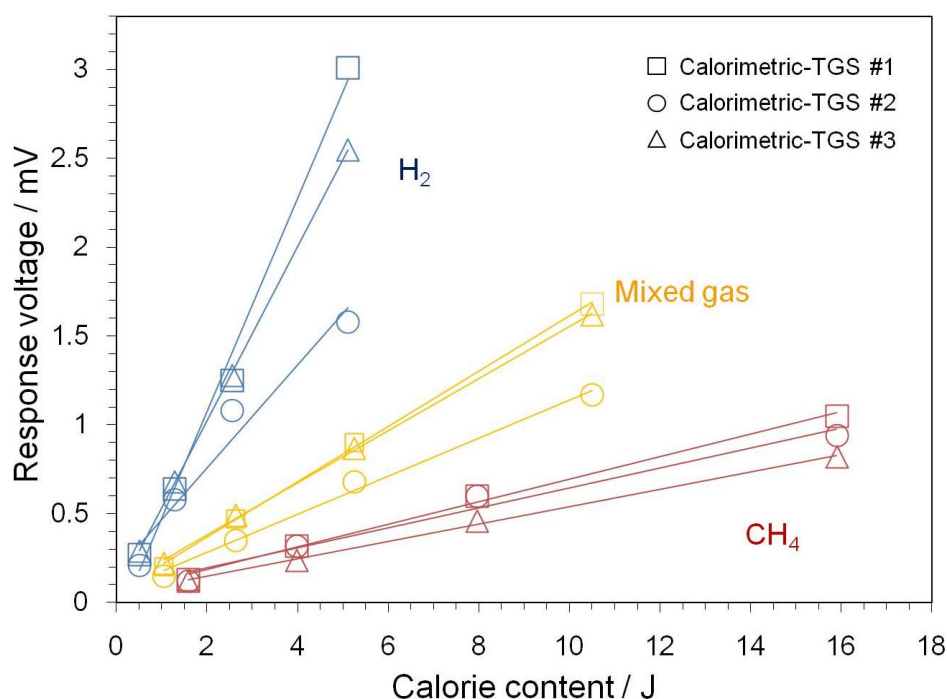
Figure 6. Schematic illustrations of the combustion mechanisms of the dual-catalyst calorimetric-TGS devices for mixed H_2 and CH_4 in air (top left and bottom left), and the expected graphs of gas calories-to-response voltages (top right and bottom right).

3.3. Responses to Combustion Calories by the Calorimetric-TGS Devices

Graphs of the observed gas combustion calories to the response voltages toward H_2, CH_4, and the mixed gases are shown in Figure 7, which were plotted using results obtained at operating temperatures of 400, 391 and 400 ℃ for the calorimetric-TGSs #1, #2 and #3, respectively. The graphs show the gas detection performance of the calorimetric-TGS devices from 200 to 2000 ppm gas in air (from 0.51 J for 200 ppm H_2 to 15.9 J for 2000 ppm CH_4), confirming the very linear responses to the calorie content. The response to the combustion heat for H_2 decreases with the Pt concentration in the Pt/α-Al_2O_3 catalyst. The response to CH_4 combustion heat increases from 0.12 to 1.05 mV in the combustion calorie range of 1.59 and 15.9 J. To date, research is limited on the detection of CH_4. Fleischer *et al.* [13] reported the detection of CH_4 using a Ga_2O_3 thin film at high temperature (300–800 ℃), which had a sensitivity of about 5 or 80 ppm to 5000 ppm CH_4 in air at 420 and 740 ℃, respectively. Sun *et al.* [14] reported that CH_4 gas burns on SnO_2 materials at temperatures above 600 ℃, and Liu *et al.* [15] reported CH_4 detection at 450 ℃. However, although CH_4 detection has been very difficult in the low temperature range (below 400 ℃), our calorimetric-TGSs successfully detected CH_4 at temperatures below 400 ℃. The responses to combustion heat, calorie content, for the mixed gases provide reasonable results with respect to the each gas (50% H_2 and 50% CH_4) in the mixture. Consideration of the thermal resolution of the calorimetric-TGS devices demonstrated that the sensor could detect 200 ppm H_2 (0.51 J) in air; thus, we can conclude that the resolution is sufficiently high for calorimetric applications. High resolution performance in the device is predicted for the detection of the heats of dilute fuel gases or for very small samplings of fuel gases.

Figure 7. Combustion heats of calorimetric-TGS devices with various catalytic combustor compositions. The operating temperatures of devices #1, #2 and #3 are 400, 391 and 400 ℃, respectively. Gas concentrations are 200, 500, 1000 and 2000 ppm for H_2, CH_4 and the gas mixture.

The calorimetric calibration of the calorimetric-TGS devices, which is an important part of their characterization, can be expressed by the following equation:

$$Q \propto \Delta V \tag{3}$$

which can be rewritten as:

$$Q = K \cdot \Delta V \tag{4}$$

where Q, K, and ΔV are the combustion heat, a response-to-combustion heat conversion factor, and the response voltage, respectively. Response-to-combustion heat conversion factors (K_{H_2}, K_{CH_4}, and $K_{Mixedgas}$) are calculated from the measurement of each gas (H_2, CH_4, and mixed gases), and the results are shown in Table 2. The calibration functions of the calorimetric-TGS devices are linear between gas concentrations of 200 to 2000 ppm for each gas as shown in the table. Although the calorimetric-TGS devices show various response-to-combustion heat conversion factors for H_2, CH_4, and the mixed gases, device #2 shows relatively smaller differences in its conversion factors for all three gas flows than the other devices.

Ideally, a calorimeter should have a constant response-to-combustion heat conversion factor for each specific gas in a fuel, showing for each data point its response to the combustion heats of the gases plotted on the same line. This study is a step toward an ideal calorimeter for reliable application. These calorimetric-TGS devices have successfully demonstrated that the H_2 combustion heat, which is easily generated at low temperature, can be reduced by up to 50% and the total observed response approaches that of CH_4 more closely. It is worth noting that the dual-catalyst calorimetric-TGS devices demonstrate reduced responses to the combustion heat of H_2 by integrating the Pt/α-Al$_2$O$_3$ catalyst at point B. Future work is planned to improve the combustion of CH_4, for example, by changing the catalyst composition or materials.

Table 2. Response-to-combustion heat conversion factors for the calorimetric-TGS devices.

Device	**K (J/mV)**		
	K_{H_2}	K_{CH_4}	$K_{Mixedgas}$
Calorimetric-TGS #1	1.6546	15.771	6.4081
Calorimetric-TGS #2	3.4524	17.874	9.3645
Calorimetric-TGS #3	2.0382	20.479	6.8084

4. Conclusions

Calorimetric-TGS devices were prepared by integrating catalyst combustors with a dual-catalyst structure (Pd/θ-Al$_2$O$_3$ and Pt/α-Al$_2$O$_3$ catalysts on the hot and cold sides, respectively). The calorimetric-TGS devices detected H_2, CH_4, and mixtures of the two with high resolution in the concentration range 200–2000 ppm (*i.e.*, the calorie range 0.51–15.9 J) and the temperature range 100–400 ℃ in air. Also, these calorimetric-TGS devices displayed both temperature- and gas

concentration-dependent responses to H_2, CH_4, and the mixed gases with constant response-to-combustion heat conversion factors (K). The calorimetric-TGS device with the 3 wt% $Pt/\alpha\text{-}Al_2O_3$ catalyst on the cold side reduced the response to H_2 combustion heat by up to 50%. Therefore, we believe that this calorimetric-TGS device is a promising, low-cost, gas calorimeter candidate with short start-up and response times, and would be appropriate for small–systems applications. However, it will be necessary to achieve greater temperature accuracy and compensate for the dependence of the temperature measurement for the device in future work, because it is of crucial importance to measure the different gases in fuels with reliability and accuracy in calorimetric applications.

Author Contributions

Woosuck Shin designed the study. Nam-Hee Park performed experiments and prepared the manuscript. All authors discussed the results and implications. Takafumi Akamatsu, Toshio Itoh and Noriya Izu provided helpful feedback commented on the manuscript at all stages.

Conflicts of Interest

The authors declare no conflict of interest.

References

1. Udina, S.; Carmona, M.; Pardo, A.; Calaza, C.; Santander, J.; Fonseca, L.; Marco, S. A micromachined thermoelectric sensor for natural gas analysis: Multivariate calibration results. *Sens. Actuat. B Chem.* **2012**, *166–167*, 338–348.
2. Gibbons, T.B.; Wright, I.G. A Review of Materials for Gas Turbines Firing Syngas Fuels; Technical Report; National Technical Information Service: Springfield, VA, USA, May 2009, pp. 6–11.
3. Shin, W.; Tajima, K.; Choi, Y.; Izu, N.; Matsubara, I.; Murayama, N. Micro thermoelectric device with ceramic combustor. *Sens. Actuat. A Phys.* **2006**, *130–131*, 411–418.
4. Houlet, L.; Tajima, K.; Shin, W.; Izu, N.; Itoh, T.; Matsubara, I. Platinum micro-hotplates on thermal insulated structure for micro-thermoelectric gas sensor. *IEEJ Trans. Sens. Micromach.* **2006**, *126*, 568–572.
5. Shin, W.; Houlet, L.F.; Nishibori, M.; Izu, N.; Itoh, T.; Matsubara, I. Fabrication of thermoelectric gas sensors on micro-hotplates. *Sens. Actuat. B Chem.* **2009**, *139*, 340–345.
6. Missal, W.; Kita, J.; Wappler, E.; Bechtold, F.; Moos, R. Calorimetric sensitivity and thermal resolution of a novel miniaturized ceramic DSC chip in LTCC technology. *Thermochim. Acta* **2012**, *543*, 142–149.
7. Hasegawa, T. Gas turbine combustion and ammonia removal technology of gasified fuels. *Energies* **2010**, *3*, 335–449.
8. Nishibori, M.; Shin, W.; Houlet, L.F.; Tajima, K.; Itoh, T.; Murayama, N.; Matsubara, I. New structural design of micro-thermoelectric sensor for wide range hydrogen detection. *J. Ceram. Soc. Jpn.* **2006**, *114*, 853–856.

9. Sasahara, T.; Kido, A.; Ishihara, H.; Sunayama, T.; Egashira, M. Highly sensitive detection of volatile organic compounds by an adsorption/combustion-type sensor based on mesoporous silica. *Sens. Actuat. B Chem.* **2005**, *108*, 478–483.

10. Nishibori, M.; Shin, W.; Izu, N.; Itoh, T.; Matsubara, I. Microheater meander configurations for combustion catalysts in thermoelectric gas sensor. *Sens. Lett.* **2010**, *8*, 1–9.

11. Wood, C. Materials for thermoelectric energy conversion. *Rep. Progress Phys.* **1988**, *51*, 459–539.

12. Choi, Y.; Tajima, K.; Shin, W.; Izu, N.; Matsubara, I.; Murayama N. Combustor of ceramic Pt/alumina catalyst and its application for micro-thermoelectric hydrogen sensor. *Appl. Catal. A Gen.* **2005**, *287*, 19–24.

13. Fleischer, M.; Meixner, H. A selective CH_4 sensor using semiconducting Ga_2O_3 thin film based on temperature switching of multigas reactions. *Sens. Actuat. B Chem.* **1995**, *24–25*, 544–547.

14. Sun, L.; Qui, F.; Quan, B. Investigation of a new catalytic combustion-type CH_4 gas sensor with low power consumption. *Sens. Actuat. B Chem.* **2000**, *66*, 289–292.

15. Liu, F.; Zhang, Y.; Yu, Y.; Xu, J.; Sun, J.; Lu, G. Enhanced sensing performance of catalytic combustion methane sensor by using Pd nanorod/γ-Al_2O_3. *Sens. Actuat. B Chem.* **2011**, *160*, 1091–1097.